Journal of Quantitative Spectroscopy & Radiative Transfer 317 (2024) 108930

Contents lists available at ScienceDirect

Journal of Quantitative Spectroscopy and Radiative Transfer

journal homepage: www.elsevier.com/locate/jqsrt

Fire monitoring and detection using brightness-temperature difference and water vapor emission from the atmospheric infrared sounder

Jason Yu [a,b], Xun Jiang [c], Zhao-Cheng Zeng [b,d], Yuk L. Yung [b,*]

[a] Viterbi School of Engineering, University of Southern California, Los Angeles, 90089 CA, USA
[b] Division of Geological and Planetary Sciences, California Institute of Technology, 1200 East California Boulevard, Pasadena, 91125 CA, USA
[c] Department of Earth & Atmospheric Sciences, University of Houston, Houston, 77004 TX, USA
[d] School of Earth and Space Sciences, Peking University, Beijing, 100871, China

ARTICLE INFO

Keywords:
Fire Detection
Atmospheric Infrared Sounder
Brightness-temperature Difference Algorithm,
Water Vapor

ABSTRACT

Radiance data from the Atmospheric Infrared Sounder (AIRS) on board NASA's Aqua satellite provide an opportunity for fire detection. As wildfires play an increasingly great role in the environments of the United States West Coast, emergency teams face an ever-challenging task of mitigation and prediction. Furthermore, the increasing rate of wildfires in the American West Coast places an ever-increasing strain on ecosystems and global climate. Of particular interest is the ability to create effective near real-time (NRT) imaging and prediction. Advances in this field can play a crucial role in assisting wildfire detection and monitoring. Typical sources for satellite fire imaging study are the Moderate Resolution Imaging Spectroradiometer (MODIS), the Visible Infrared Imaging Radiometer Suite (VIIRS), the Advanced Very High Resolution Radiometer (AVHRR), and the Spinning Enhanced Visible and Infrared Imager (SEVIRI) instruments, but we present AIRS as complementary to these instruments with a new method of hotspot analysis. In this study, we propose a new method of fire detection by using AIRS's cloud-cleared radiance to detect hotspots and find new applications for this method of retrieval. We present the fire detection algorithm and initial assessments showing AIRS's ability to detect fires. In addition, we notice that there is more water vapor from the surface to the upper troposphere during the fire event as a result of biomass burning and an increase in air temperature.

Key Points

- AIRS is a candidate for a fire incident detection and monitoring system
- The brightness-temperature difference algorithm aids in fire anomaly detection
- More water vapor is seen from the surface to the upper troposphere during the fire

Data availability

Data will be made available on request.

1. Introduction

As of September 2020, the Moderate Resolution Imaging Spectroradiometer (MODIS) and the Visible Infrared Imaging Radiometer Suite (VIIRS)—long-time standards for radiometric remote sensing for fire detection—have recorded over 15,000 cumulative fire detections in the United States West Coast in 2020 alone, spanning a region of over five million total burned acres [1]. Surpassing the previous record of just under 10,000 detections by September in 2018, 2020 has been a record wildfire season for California and nearby states. In California alone, the August 2020 lightning wildfires, including the August Complex fire, Santa Clara Unit (SCU) Lightning Complex fires, and the Creek fire burned a combined total of over two million acres.

Prior to 2020's wildfire season, 2018 held the record for most destructive and most costly wildfires in California, largely in part due to November 2018's Camp Fire, which burned nearly 154,000 acres and resulted in over $16 billion in total losses [2] —the current

* Corresponding author.
E-mail address: yly@caltech.edu (Y.L. Yung).

https://doi.org/10.1016/j.jqsrt.2024.108930
Received 27 March 2023; Received in revised form 4 February 2024; Accepted 4 February 2024
Available online 6 February 2024

record-holder for costliest wildfire in global history. Both the 2017 and 2018 wildfire seasons held the record for the two largest wildfire incidents (Mendocino Complex Fire 2018, Thomas Fire 2017), a record shattered by the 2020 wildfire season, which displaced the two record holders to 2nd largest and 7th largest, respectively. The 2020 season has seen four of the five largest California wildfires, two of the top ten most destructive California wildfires, and one of the top five deadliest California wildfires—more than any other fire season in California [3]. As noted from recent climate trends, anthropogenic (human-caused) climate change is likely to cause warming atmospheres and, with each subsequent fire season, a greater likelihood of wildfire incidents [4]. With the ever-increasing threat of wildfire incidents in a progressively warming climate, the need for satellite-based imagery for fire detection in the absence or incapacitation of aerial or ground detection sources has never been higher. The 2020 wildfire season in the western U.S. has shown the effectiveness of satellite-based detection systems, where the number of fires is in excess of aerial detection planes or land-based sensors available. The lack of fire detection infrastructure in these remote locations raises the ever-pressing need for near real-time (NRT) fire detection without immense infrastructure investment.

Since the 1998 seminal paper on satellite-based burn monitoring [5], MODIS has been used by researchers as the primary driver for daily fire imaging. It has since been adapted into NASA's Earth Observing System Data and Information System (EOSDIS), where it has advanced global fire location systems [6] and other satellite-based fire detection algorithms [7]. The Atmospheric Infrared Sounder (AIRS) instrument onboard the Aqua satellite [8] was never intended as a remote sensing tool for fire monitoring, but its twice-daily local retrievals and large swaths make it a good candidate as a continuous fire monitoring and inspection tool.

Intended as a state-of-the-art instrument for cloud, atmospheric, and land/ocean measurement, AIRS's primary use has been for atmospheric and oceanographic climate monitoring. As such, the AIRS data have never been used for fire detection. We present a wildfire detection method based on AIRS's cloud-cleared radiance product and establish the instrument's potential as a complement to other satellite-based fire imaging.

There are two primary aims in this study: (1) to establish AIRS as complementary to current multi-spectral instruments such as MODIS and VIIRS for use in fire detection and monitoring through a combination of its radiance and water vapor products; and (2) to establish a new method of hotspot anomaly and fire detection/progression with brightness-temperature.

2. Methods and fire locations

The AIRS instrument, on board NASA's Aqua satellite, provides the cloud-cleared radiance product (in units of $mW/m^2/sr/cm^{-1}$) at a spatial resolution of 45 km across 2378 infrared channels—the instrument measures between a lower-bound wavenumber of 650 cm^{-1} and an upper-bound of 2675 cm^{-1} [9,10]. AIRS records data in six-minute granules, each featuring up to 1350 total retrievals per granule. Each granule records a 1500 km-wide swath.

To validate AIRS's capability for fire detection, we analyze cloud-cleared radiance data from various past fire locations in 2017 and 2020, for regions of approximately 44 to 100 kms across. In this study, we select only AIRS data during nighttime intervals to minimize radiance interference from sunlight and other diurnal cycle variations (AIRS has daytime and nighttime swaths). The AIRS instrument on the Aqua satellite contains 2378 channels on its cross-track scanner and a 13.5 km field of view (FOV) at nadir. We also disregard all data flagged by the instrument's quality control parameter (radiances_QC) as "do not use" [11]. For this study, we investigate data directly from the instrument with no additional re-gridding; we avoid further interpolation and find the native resolution provided by AIRS to be sufficient for this study. Fire Radiative Power data from MODIS are also used to generate burn maps for continuity comparison with AIRS results.

Three primary locations were selected for analysis: the 2017 Nuns fire (San Francisco Bay area), the 2020 Bobcat fire (Los Angeles area), and the 2020 Creek fire (Fresno/Madera County). Fire details and their respective burn statistics for the locations used in this study are summarized in Table 1.

Using AIRS version 7 level 2 cloud-cleared radiance data, we first convert blackbody radiance ($mW/m^2/sr/cm^{-1}$) to brightness-temperature in degrees Kelvin (K)—the conversion is derived from the Planck Function and given by Equation 1.

$$\boldsymbol{T}(\boldsymbol{\nu}, \boldsymbol{B}) = \frac{\boldsymbol{c}_2 \boldsymbol{\nu}}{\ln(\boldsymbol{c}_1 \boldsymbol{\nu}^3 / \boldsymbol{B} + 1)} \tag{1}$$

where T is brightness-temperature, B is radiance, ν is wavenumber, c_1 is $1.191 \times 10^{-5} Wm^2 sr^{-1}$, and c_2 is 1.439 m K.

To determine locations with potential hotspots, we compute the difference of brightness-temperature between those corresponding to high wavenumbers and low wavenumbers. First, we average the brightness-temperature from approximately 40 channels in the low wavenumber region (from 1221 cm^{-1} to 1241 cm^{-1}). Then, we compute the analogous average for approximately 35 channels in the high wavenumber region (from 2606 cm^{-1} to 2623 cm^{-1}). Finally, we compute the brightness-temperature difference between the average temperatures for the high-wavenumber region and the low-wavenumber region to produce a temperature-difference index. The variation in the brightness temperature between high and low wavenumber regions is due to different Plank function sensitivities to the same degree of temperature change. The areas with large differences with respect to their surroundings indicate potential hotspot regions. We also analyze the timeseries of brightness-temperature difference. To explore the influence of fires on water vapor, we analyze AIRS Version 7 water vapor mass mixing ratio [11,12] before and during the fire event. AIRS Version 7 water vapor mass mixing ratio data are available from August 2002 to the present with a spatial resolution of 13.5 km at nadir. AIRS water vapor mass mixing ratio data agree reasonably well with the Microwave Limb Sounder [12] and the European Centre for Medium-Range Weather Forecasts[11]. Previous studies (e.g., [13,14]) found that water vapor can be released to the atmosphere during the fire by chemical reactions and evaporation. In this paper, we investigate the impact of fires on the vertical profiles of water vapor mass mixing ratio using AIRS Version 7 data. Results of AIRS water vapor mass mixing ratio are compared to those from the Modern-Era Retrospective analysis for Research and Applications, Version 2 (MERRA-2) Reanalysis data [15]. MERRA-2 is a NASA atmospheric data reanalysis using the Goddard Earth Observing System Data Assimilation System Version 5 (GEOS-5) [15].

Burn area data from the MODIS instrument for the same incident dates are also listed in Table 1. We estimate geospatial burn fire incident spots by computing the brightness-temperature difference for each available point from the AIRS instrument within 40–100 kms of the fire location, depending on the fire's size. In our investigation, we found that brightness-temperature difference anomalies above 7 K matched with known fire incidents. Therefore, we plot the (longitude, latitude) pairs of AIRS data points only if the region's brightness-temperature difference exceeds 7 K. MODIS data used in this study to validate the AIRS results are taken from its fire radiative power (FRP) product. We select data matching a confidence range exceeding 33% (corresponding to a nominal or "high" confidence reading), as reported by Giglio et al. [7].

The Moderate Resolution Imaging Spectroradiometer (MODIS) onboard the Aqua and Terra satellites provide a benchmark fire radiative power (FRP) estimate using two broad thermal bands at around 4 μm and 11 μm with high spatial resolution (~1 km) observation. Unlike the broadband observations of MODIS, AIRS captures the full spectral range with high spectra resolution from the mid-IR to thermal-IR from 3.75 to 15.4 μm, however, with a coarse spatial resolution (~13.5 km). An

Table 1
Fire details and their respective burn statistics.

Fire name	Origin	Start date	Containment date	Acres burned	Area of Interest	
					Longitude	Latitude
Nuns	Sonoma Valley, California	October 8, 2017	October 30, 2017	245,000	−122.25°	38.37°
Bobcat	Angeles National Forest, California	September 6, 2020	December 18, 2020	115,796	−117.87°	34.24°
Creek	Fresno/Madera County, California	September 4, 2020	December 24, 2020	379,895	−119.26°	37.19°

advantage of the spectrally resolved data by AIRS will enable better quantification of the fine structure of blackbody radiation emitted by wildfires. Also, there are almost two decades of global AIRS observations available. The independent dataset to be produced from AIRS will enable us to verify the widely used estimates from MODIS.

3. Results

We have analyzed AIRS version 7 cloud-cleared radiance data before, during, and after the Nuns fire. Results are shown in Fig. 1. The radiance signal at the outset of the fire on October 8, 2017 (indicated by the red curve) is considerably higher than those before or after the fire incident (shown by the blue and black curves, respectively). We have fitted the AIRS radiance baseline using a two-blackbody radiation model. A similar model was presented by Green [16]. Here we try to fit the AIRS observation using a two-blackbody radiation model with emissivity assumed to be one. The equation is given as

$$B = (1-\eta)B(T_s) + \eta B(T_f) \quad (2)$$

where the function $B(T)$ is the Planck's function for blackbody emission at temperature T for the given wavenumber; $T_s and T_f$ are the temperature for the areas with no fire and with fire, respectively. η is the fire fractional area for the footprint of AIRS instrument. Temperature for the areas with fire, temperature for the areas without fire, and the fire fractional area are provided for the two-blackbody radiation model. Using the simple two-blackbody radiation model, we can fit the AIRS observation baseline well (See Figure S1 in the Supplementary Materials). The two-blackbody radiation model demonstrates that fires can influence the radiance at different wavenumber regions. Brightness-temperature converted from AIRS version 7 cloud-cleared radiance before, during, and after the Nuns fire are shown in Fig. 2. The brightness-temperature before/after the fire are noticeably lower than that during the fire (in the ~750–1250 and ~2250–2700 cm^{-1} regions). Furthermore, brightness-temperature shows the sharp rise in temperature at the 2500 cm^{-1} wavenumber region and beyond. AIRS clearly detects the presence of a temperature anomaly, corresponding to the outset of the Nuns fire on October 9. Similar analysis is applied to the

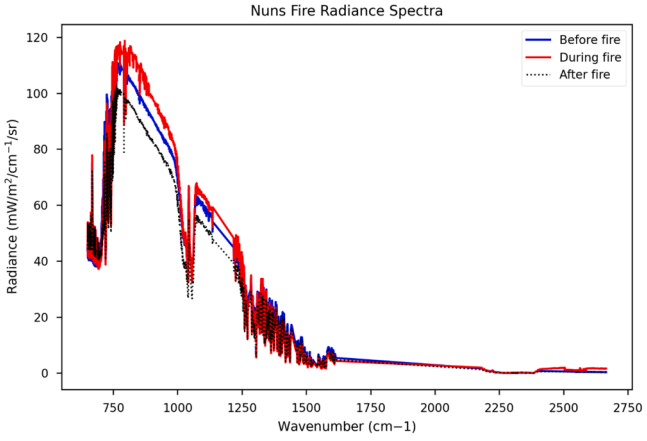

Fig. 1. AIRS radiance spectra for October 8 (before the fire), October 9 (during the fire), and October 13, 2017 (after the fire) at the Nuns fire location.

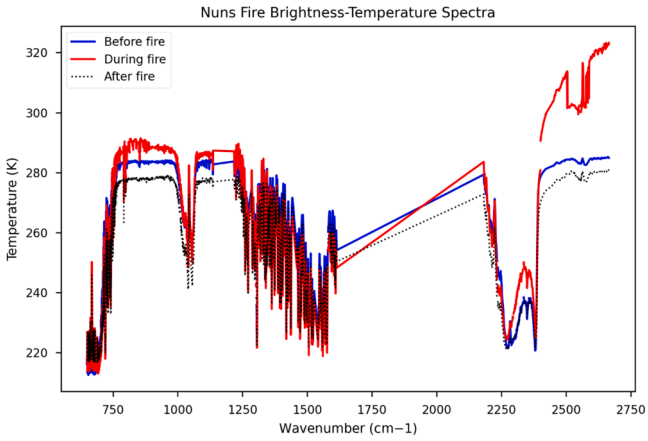

Fig. 2. AIRS brightness-temperature for October 8 (before the fire), October 9 (during the fire), and October 13, 2017 (after the fire) at the Nuns fire location.

2020 Bobcat fire and 2020 Creek fire. As seen in Figures S4-S5 in the Supplementary Materials, brightness-temperature is higher during the fire than those before or after fire for all fire events over the high wavenumber region (2250–2700 cm^{-1}).

The sharply increasing brightness-temperature in the high wavenumber regions is what we are most interested in. As is consistently found across all fires tested in this study, we find that the temperature difference between the high wavenumber region and the low wavenumber region produces a new scalar value, which allows us to create an index for potential fire incidents. In this study, we elect to use the low wavenumber region from 1221 cm^{-1} to 1241 cm^{-1} and the high wavenumber region from 2606 cm^{-1} to 2623 cm^{-1} due to its minimal interference from other gases' absorptions, which may cause large varying results.

The MODIS burn incident map for Oct. 9, 2017 (outset of the Nuns fire) is shown in Fig. 3a. For comparison, we calculate the AIRS brightness-temperature difference between high and low wavenumber regions for Oct. 9, 2017. All locations with brightness-temperature difference higher than 7 K are highlighted as red dots in Fig. 3b. As shown in Fig. 3, AIRS can detect anomalous burn regions during the Nuns fire at its appropriate geographic location. We replicate this analysis for the remainder of the fires in Table 1; figures are provided in the Supplementary Materials. As shown in Figures S6-S7, AIRS brightness-temperature difference can be used to detect the fire locations for all fire events.

In addition to detecting the fire locations using AIRS data, we also explore the temporal variation of the AIRS brightness-temperature difference for the Nuns fire. The AIRS brightness-temperature difference timeseries, shown in Fig. 4, clearly shows the first signal anomaly on the evening of Oct. 9, 2017, corresponding to the first day of the Nuns fire. We also investigate temporal variations of the brightness-temperature difference for other fires. Results are shown in Figures S8-S9 in the Supplementary Materials. In general, brightness-temperature differences before the initial outbreak of the fire are less than 2–3 K. At the outset of a fire, the temperature difference rises to greater than 5–7 K. In more extreme and larger fires, the temperature differences can reach several dozen degrees Kelvin.

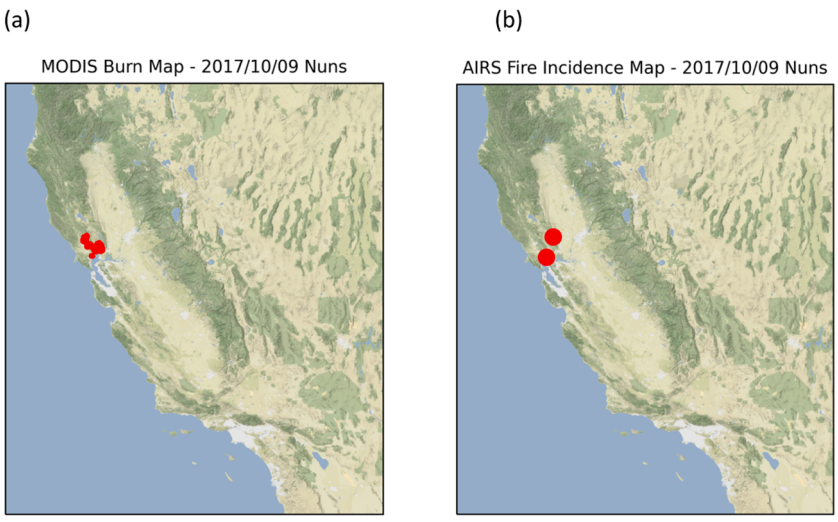

Fig. 3. (a) MODIS burn incident map on October 9, 2017 (start of the Nuns fire) showing burn area in the region surrounding the Sonoma Valley (b) AIRS temperature difference fire incident map on October 9, 2017 for the Nuns fire.

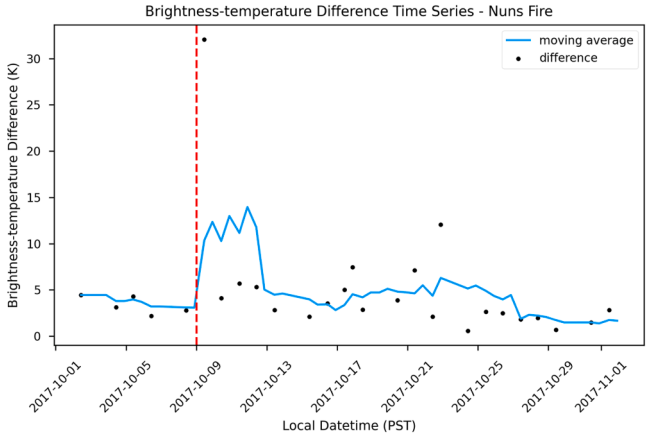

Fig. 4. AIRS brightness-temperature difference time series (blue line). Red dashed line highlights the outset of the Nuns fire.

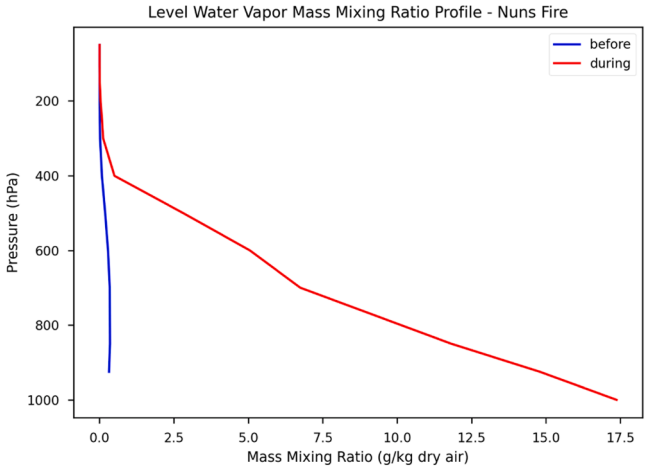

Fig. 5. AIRS water vapor mass mixing ratio vertical profiles before and during the Nuns fire. Units are g/kg.

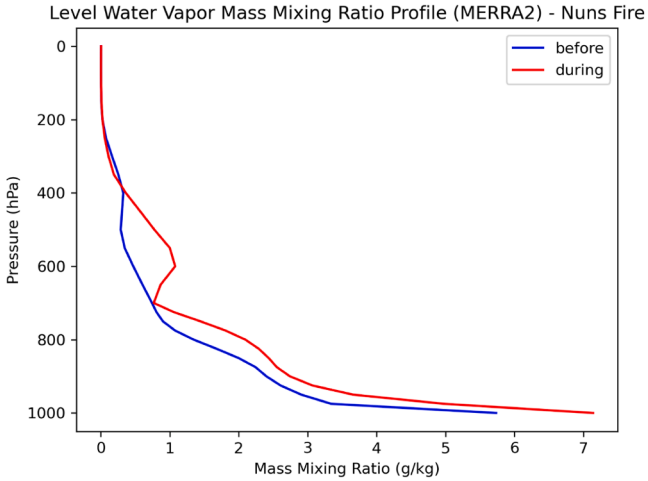

Fig. 6. MERRA-2 model water vapor mass mixing ratio vertical profiles before and during the Nuns fire. Units are g/kg, converted from specific humidity.

As shown in Figs. 1 and 2, large absorption features due to water vapor in 1250–1500 cm^{-1} and 2500–2650 cm^{-1} regions can be found. To better understand the variations of water vapor before and during the fire, we calculate the vertical profiles of AIRS Version 7 water vapor mass mixing ratio before and during the Nuns fire (Fig. 5). Water vapor mass mixing ratio is exceptionally low before the fire (blue curve). There is more water vapor from the surface to the upper troposphere during the fire (red curve), which is a result of releasing water vapor from biomass burning [13,14] and increasing air temperature. Previous studies (e.g., [13,14]) found that water vapor can be released to the atmosphere through chemical reactions and evaporation during the combustion process. Air temperature increases during the fire, resulting in more water vapor in the air following the Clausius-Clapeyron equation (e.g., [17]). The updrafts induced by the fires can further increase transport of water vapor from the surface to the upper-troposphere.

Compared to water vapor mass ratios from the MERRA-2 Reanalysis data [15], water vapor results from AIRS show larger variability than those from the MERRA-2. MERRA-2 results (Fig. 6) also show stronger water vapor presence during the fire than before the fire, which match expected observations from AIRS. However, MERRA-2 data have difficulties in capturing low water vapor mass mixing ratio before the fire. As AIRS more strongly shows the release of water vapor than MERRA-2 does, water vapor observations from AIRS are better equipped to

supplement fire detection with its unique fire radiative product. We also investigate vertical profiles of water vapor mass mixing ratios before and during the 2020 Bobcat fire and the 2020 Creek fire. Results are shown in Figures S10-S13 in the Supplementary Materials. As shown in AIRS water vapor mass mixing ratio data, there is more water vapor during the fire than before the fire for all fire events (Figure S10, S12). The difference of MERRA-2 water vapor before and during the fire is not as clear as AIRS observations, which might be related to the coarse spatial resolution of MERRA-2 and relatively poor performance in simulating the horizontal and vertical mixings in the model.

4. Conclusion

This study presents a fire incident detection method using blackbody radiance data from infrared remote sensing tools. While AIRS data are used primarily for fine-tuning weather forecasting and modeling (with major emphasis in atmospheric and greenhouse gas sciences), we present the case for multi-purposing existing weather satellites like AIRS as additional fire incident sensors using radiance signals. Remote sensing tools which utilize a wide range of infrared channels to record blackbody radiance can use our algorithm to derive a new active fire product with little cost overhead. Our method of retrieval, which involves a simple scalar conversion from blackbody radiance to brightness-temperature and difference in brightness-temperatures between high- and low-wavenumber intervals, has potential for adding new features to existing remote sensing tools for near real-time fire detection and monitoring at an accuracy and confidence level that leaves AIRS uniquely situated to detect, monitor, and validate current spectroradiometry sensor readings. Though AIRS's field of view is fairly large, our brightness-temperature difference method of fire detection performs well for three prominent case studies of fires in the western United States. We expect that this method of retrieval may be equally as (or more) effective if applied to sensors with finer spatial resolutions, as more data retrievals should be available for processing. Smaller, more frequent swaths allow for finer detection of smaller fires and provide greater confidence for larger ones.

Just as wildfires become a growing threat to the world, the need for more omnipresent fire detection monitoring and detection tools rises. In regions where aerial and ground monitoring or existing satellite fire detection products are not available, the value of repurposed, aging satellites (which ultimately allow for broader coverage of wildfire-prone areas) increases. With a greater array of remote sensing tools for fire detection available, fire agencies will have greater chance of picking up and verifying remote fires during peak wildfire seasons, when resources are scarce. Though MODIS and VIIRS are expected to continue service, adding additional satellite fire products give agencies yet another detection option. We believe that the AIRS (cloud-cleared radiance and water vapor products) is a foundational example for driving similar research on existing products. The algorithm we have presented can serve as a wildfire detection method onboard the Aqua AIRS instrument. Similar analyses can be applied to other instruments (e.g., Infrared Atmospheric Sounding Interferometer (IASI) and Cross-track Infrared Sounder (CrIS)) in the future.

CRediT authorship contribution statement

Jason Yu: Data curation, Formal analysis, Investigation, Methodology, Software, Validation, Visualization, Writing – original draft, Writing – review & editing, Conceptualization. **Xun Jiang:** Conceptualization, Data curation, Formal analysis, Investigation, Methodology, Project administration, Software, Supervision, Validation, Visualization, Writing – original draft, Writing – review & editing. **Zhao-Cheng Zeng:** Formal analysis, Investigation, Methodology, Software, Validation, Writing – review & editing. **Yuk L. Yung:** Conceptualization, Supervision, Writing – review & editing.

Declaration of competing interest

The authors declare that they have no known competing financial interests or personal relationships that could have appeared to influence the work reported in this paper.

Data availability

Data will be made available on request.

Acknowledgements

The authors thank the referees and the editor for their time and constructive suggestions. Y. L. Yung is supported by the NASA OCO-2 project. X. Jiang is supported by NASA ROSES Cassini Data Analysis Program. AIRS Version 7 Level 2 cloud-cleared radiance can be downloaded from https://airsl2.gesdisc.eosdis.nasa.gov/data/Aqua_AIRS_Level2/AIRS2CCF.7.0/. AIRS Version 7 water vapor mass mixing ratio data can be downloaded from https://airsl2.gesdisc.eosdis.nasa.gov/data/Aqua_AIRS_Level2/AIRS2RET.7.0/. MODIS burn data can be downloaded from https://lpdaac.usgs.gov/products/mcd64a1v006.

Supplementary materials

Supplementary material associated with this article can be found, in the online version, at doi:10.1016/j.jqsrt.2024.108930.

References

[1] Blacki Migliozzi, N.P., McCann, A., 2020. Record wildfires on the west coast are capping a disastrous decade. Retrieved from Record Wildfires on the West Coast Are Capping a Disastrous Decade: https://www.nytimes.com/interactive/2020/09/24/climate/fires-worst-year-california-oregon-washington.html.

[2] Reyes-Velarde, A., 2019. *California's Camp fire was the costliest global disaster last year, insurance report shows*. Retrieved from California's Camp fire was the costliest global disaster last year, insurance report shows: https://www.latimes.com/local/lanow/la-me-ln-camp-fire-insured-losses-20190111-story.html.

[3] Cal Fire, 2020. Top 20 largest California wildfires. Retrieved from https://www.fire.ca.gov/media/4jandlhh/top20_acres.pdf.

[4] Higuera PE, Abatzoglou JT. Record-setting climate enabled the extraordinary 2020 fire season in the western United States. Glob Chang Biol 2020;27:1–2. https://doi.org/10.1111/gcb.15388.

[5] Kaufman YJ, Justice CO, Flynn LP, Kendall JD, Prins EM, Giglio L, et al. Potential global fire monitoring from EOS-MODIS. J Geophys Res: Atmos 1998;103:32215–38.

[6] Ramapriyan HK. Development, Operation and Evolution of EOSDIS–NASA's major capability for managing Earth science data. In: CENDI/NFAIS Workshop on Repositories in Science & Technology: Preserving Access to the Record of Science. 30; 2011. p. 2011.

[7] Giglio L, Descloitres J, Justice CO, Kaufman YJ. An Enhanced Contextual Fire Detection Algorithm for MODIS. Remote Sens Environ 2003;87:273–82. https://doi.org/10.1016/s0034-4257(03)00184.

[8] Aumann HH, Chahine MT, Gautier C, Goldberg M, Kalnay E, McMillin L, Revercomb H, Rosenkranz PW, Smith WL, Staelin DH, Strow L, Susskind J. AIRS/AMSU/HSB on the aqua mission: design, science objectives, data products and processing systems. IEEE Trans Geosci Remote Sens 2003;41:253–64. https://doi.org/10.1109/TGRS.2002.808356.

[9] Susskind J, Barnet CD, Blaisdell JM. Retrieval of atmospheric and surface parameters from AIRS/AMSU/HSB data in the presence of clouds. IEEE Trans Geosci Remote Sens 2003;41:390–409. https://doi.org/10.1109/tgrs.2002.808236.

[10] Susskind J, Barnet C, Blaisdell J, Iredell L, Keita F, Kouvaris L, et al. Accuracy of geophysical parameters derived from Atmospheric Infrared Sounder/Advanced Microwave Sounding Unit as a function of fractional cloud cover. J Geophy Res 2006:111. https://doi.org/10.1029/2005jd006272.

[11] Thrastarson HT, Manning E, Kahn B, Fetzer EJ, Yue Q, Wong S, et al. AIRS/AMSU/HSB version 7 level 2 product user guide. Pasadena, CA, USA: Jet Propulsion Laboratory, California Institute of Technology; 2020.

[12] Fetzer EJ, Read WG, Waliser D, Kahn BH, Tian B, Vomel H, et al. Comparison of upper tropospheric water vapor observations from the Microwave Limb Sounder and Atmospheric Infrared Sounder. J Geophys Res 2008;113. https://doi.org/10.1029/2008JD010000.

[13] Parmar RS, Welling M, Andreae MO, Helas G. Water vapor release from biomass combustion. Atmos Chem Phys 2008;8:6147–53.

[14] Potter BE. The role of released moisture in the atmosphere dynamics associated with wildland fires. Int J Wildland Fire 2005;14:77–84.

[15] Gelaro R, McCarty W, Suárez MJ, Todling R, Molod A, et al. The modern-era retrospective analysis for research and applications, Version 2 (MERRA-2). Am Meteorol Soc 2017;30:5419–54. https://doi.org/10.1175/JCLI-D-16-0758.1.
[16] Green RO. Estimating the expressed temperature and fractional area of hot lava at the Kilauea Vent with AVIRIS spectral measurements. In: *Proc. Tenth JPL Airborne Earth Science Workshop*, JPL Publication 02-1. Jet Propulsion Laboratory; 2001.
[17] Santer BD, Mears C, Wentz FJ, Taylor KE, Gleckler PJ, Wigley TML, et al. Identification of human-induced changes in atmospheric moisture content. Proc Natl Acad Sci USA 2007;104:15248–53. https://doi.org/10.1073/pnas.0702872104.